

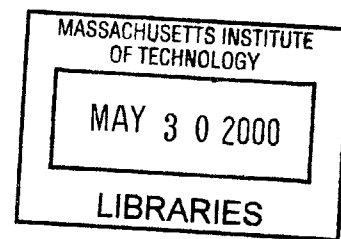
ENG

DESIGN OPTIMIZATION OF PARABOLIC ARCHES SUBJECT TO NON-UNIFORM LOADS

by

Lavina H. Sadhwani

Bachelor of Science in Civil Engineering
University of Illinois at Urbana-Champaign
May 1998



SUBMITTED TO THE DEPARTMENT OF CIVIL AND ENVIRONMENTAL ENGINEERING IN
PARTIAL FULFILLMENT OF THE REQUIREMENTS FOR THE DEGREE OF

MASTER OF ENGINEERING
IN CIVIL & ENVIRONMENTAL ENGINEERING

at

MASSACHUSETTS INSTITUTE OF TECHNOLOGY
June 2000

© 2000 Lavina H. Sadhwani
All Rights Reserved.

*The author hereby grants MIT permission to reproduce and distribute publicly paper
and electronic copies of this thesis document in whole or in part.*

Signature of Author

Department of Civil and Environmental Engineering
May 5, 2000

Certified by

Jerome J. Connor
Professor of Civil and Environmental Engineering
Thesis Supervisor

Accepted by

Daniele Veneziano
Chairman, Departmental Committee on Graduate Studies

DESIGN OPTIMIZATION OF PARABOLIC ARCHES SUBJECT TO NON-UNIFORM LOADS

by

Lavina H. Sadhwani

Submitted to the Department of Civil and Environmental Engineering
on May 5, 2000 in Partial Fulfillment of the Requirements for the Degree of
Master of Engineering in Civil and Environmental Engineering

Abstract

Arch structures have been used for centuries in various types of structural systems, particularly buildings and bridges. Arches are characterized by the ability to carry load primarily through axial action. An arch shape can be optimized such that the design load pattern is carried by purely axial action. If the load pattern on the optimized arch differs from the design loading, bending stresses develop in the arch. Load carrying mechanisms that resist load through bending are less efficient than systems that resist load through axial action. An active control system on an arch can be used to reduce the bending stresses in an arch. Control forces, and resulting moments are applied to counteract moments produced various other load combinations. The actuator, a component of the active control system, imposes counteracting control moments on the arch to limit the resultant moment forces in the arch to a pre-defined limit.

This thesis includes a description of basic arch theory; specifically, a description of various types of arches, force equilibrium equations for arch structures, and the theory behind design optimization of arch shapes for a design load pattern are presented. Additionally, the fundamentals of active control systems, including components of the system and a basic algorithm are discussed. A case study is then utilized to demonstrate that an arch structure enabled with an active control system can carry all load patterns mainly through axial action.

Thesis Supervisor: Jerome J. Connor

Title: Professor of Civil and Environmental Engineering

ACKNOWLEDGEMENTS

Writing this thesis would have taken a lot longer and been a lot more difficult if it wasn't for a few people who provided me with guidance and support, both professionally and personally:

Professor J.J.Connor, for his guidance and advice. More importantly, for revitalizing my enthusiasm for my career in structural engineering.

Emma Shepherdson, for helping me get started.

Frank, D.J. , and Brant, my eternal appreciation for listening to my continuous nagging and whining and for helping me with my formatting issues.

George Kokosalakis, for his assistance with the MATLAB program.

My family, for their continuous support and encouragement.

Table of Contents

Abstract	2
1.0 Arch Structures	6
1.1 Types of Arches	7
1.2 Arch Theory	8
2.0 Funicular Method of Arch Design	11
3.0 Disadvantages of Traditional Arch Design	12
4.0 Active Control	13
4.1 Components of Active Control System	13
4.2 Actuator Technology	15
4.3 Active Control Algorithm	16
5.0 Active-Controlled Arch Structure	18
6.0 Design of Proposed Charles River Crossing Bridge Arch	19
6.1 Introduction	19
6.2 Loads	20
6.2.1 Superstructure Loads	21
6.2.2 Self-weight	23
6.3 Funicular method	24
6.3.1 Determination of Constraints	24
6.3.2 Determination of optimal arch shape	25
6.4 Computer Model	25
6.5 Optimized Arch Shape	27
6.6 Discussion of Design Stresses	28
7.0 Design of Active Control System	29
7.1 Configuration of Actuators	29
7.2 Active Control Algorithm	30
7.3 Results of Active Control Algorithm	31
8.0 Conclusion	34

Table of Figures

Figure 1: New River Gorges Bridge..... 6

Figure 2: Natchez Bridge 7

Figure 3: Oudry Mesly pedestrian bridge..... 8

Figure 4: Typical Arch 9

Figure 5: Equilibrium Force Equations for an Arch..... 9

Figure 6: Components of an Active Control System..... 14

Figure 7: Three-rod Actuator scheme 16

Figure 8: Proposed Charles River Crossing Bridge 19

Figure 9: SAP2000 Model of Arch..... 23

Figure 10: Required Geometric Dimensions for Arch..... 24

Figure 11: Optimized Arch Shape 27

Figure 12: Moment Diagram of Arch under Design Load Combination (1)..... 28

Figure 13: Moment Diagram of Arch under Critical Load Combination (3)..... 28

Figure 14: Interaction Diagram for Critical Section..... 29

Figure 15: Proposed Actuator Scheme on Arch..... 30

Figure 16: Graph of Critical Design Moments (M_d) and Target Control Moment Distributions (M_c^)*..... 31

Figure 17: Graph of resulting Control Moments (M_c) and sum of moments on structure (e)..... 32

Figure 18: Interaction Diagram of Critical Section of Arch..... 32

1.0 Arch Structures

The first true arch structure was built approximately 44 centuries ago. However, it was not until 44 centuries after the construction of the first arch that the mechanics of arches was completely understood and formulated in the elastic theory of arches (Spofford, 1937). The enduring use of arches in civil engineering structures is attributed to the aesthetic appeal and the structural efficiency of the system (Melbourne, 1995). The first constructed arches were made of masonry. With masonry construction, the longest arch structure spanned 300 feet. With the advent of more sophisticated materials, specifically steel and reinforced concrete, arch spans have increased (Spofford, 1937). The New River Gorges Bridge, is a 1700 feet metal arch bridge located in West Virginia; currently, it is the longest constructed arch (Figure1). The longest concrete arch bridge is located in Krk, Croatia and spans 1280 feet. The Natchez Bridge, is the longest concrete arch bridge in the Unites States; it is located in Franklin, Tennessee and consists of two spans, with the longer of the two arches spanning 582 feet (Figure2).

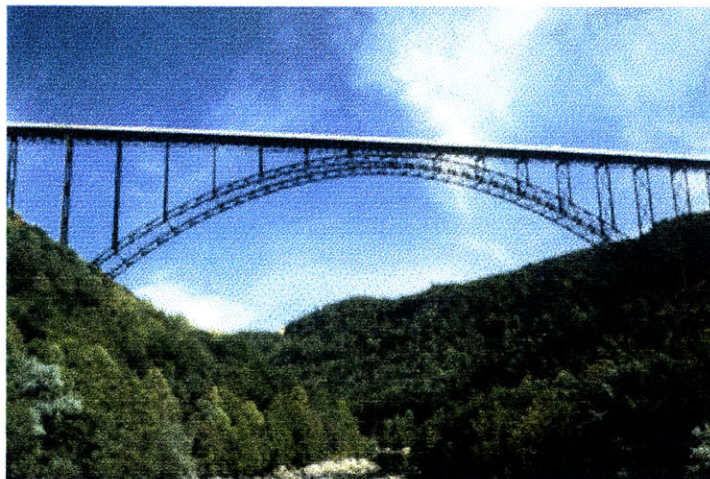


Figure 1: New River Gorges Bridge

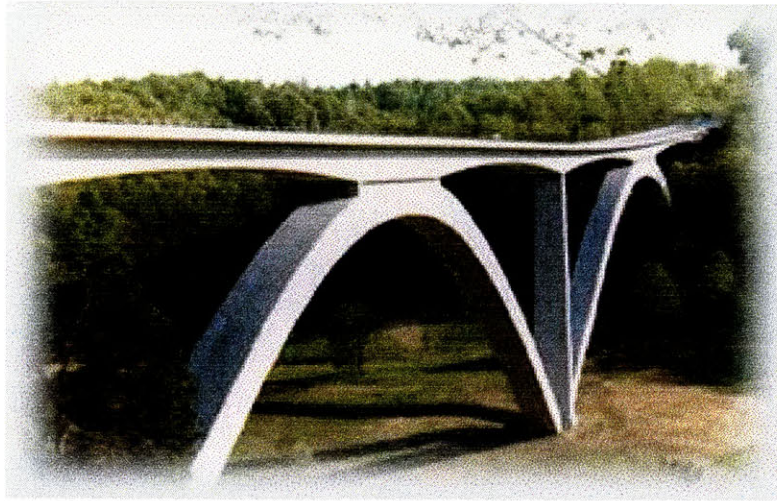


Figure 2: Natchez Bridge

1.1 Types of Arches

There are three basic types of arches, a hingeless (fixed) arch, a two-hinged arch, and a three-hinged arch. Older masonry arches have fixed supports at each base. The corresponding six unknown reactions make fixed arches statically indeterminate structures. The use of modern construction materials has made the possibility of structural determinate arches a viable alternative. A three-hinged arch incorporates a hinge at the crown of the structure in addition to hinges at the supports. The advantage of three hinged arches is they are statically determinate and can be solved through equations developed by the elastic theory; however, arches with fixed pinned supports are less stiff than structures with fixed supports. A two-hinge arch, which is also statically determinate, incorporates hinges at the supports, thereby preventing any moments from developing at the supports. For the special case where the arch loading and configuration are perfectly symmetrical, all types of arches can be also be solved through elastic equations. (Spofford, 1937)

A tied arch, incorporates an additional tension member that (typically) spans between the abutments. This member resists the horizontal thrust, thus the foundation needs only to resist vertical reactions. The tension tie must provide sufficient stiffness and prevent the arch from displacing excessively.

Most constructed arches consist of an arch spanning below the point of load application. More recent arch structures have incorporated the arch above the point of load application. The Oudry Mesly pedestrian bridge in Paris, France is an example of such a structure (Figure 3). The rationale behind the placement of the arch is related to the desired aesthetics and allowable clearances.

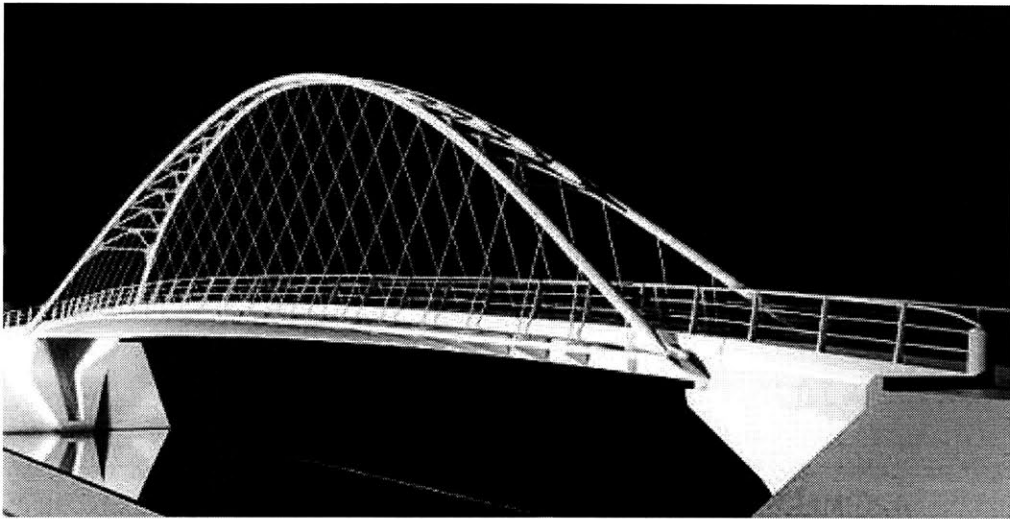


Figure 3: Oudry Mesly pedestrian bridge

1.2 Arch Theory

The distinguishing feature of an arch relative to other load carrying systems is that it carries vertical loads primarily through axial action, and not flexure. Axial action is a preferred load resisting mechanism since it makes the most efficient use of the construction material. Figure 4 demonstrates a typical arch, including the pertinent features. The arch shown in Figure 4 is a two-hinged arch. Governing force equilibrium equations for arches are shown below Figure 5.

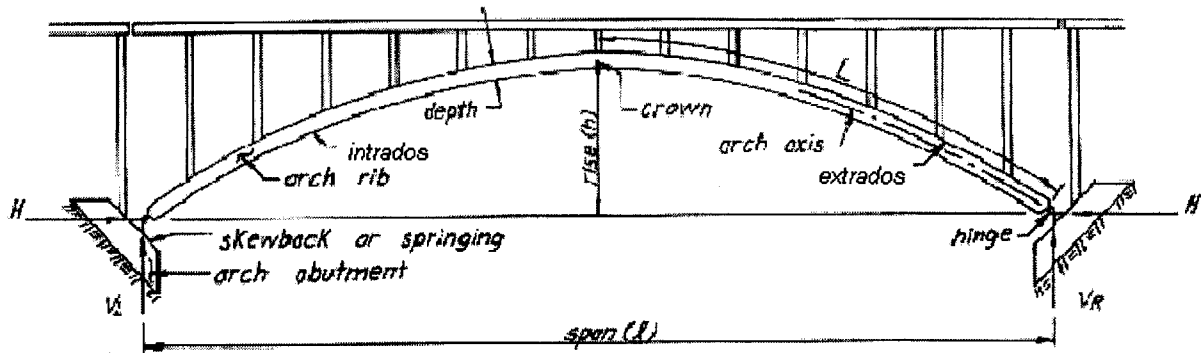


Figure 4: Typical Arch

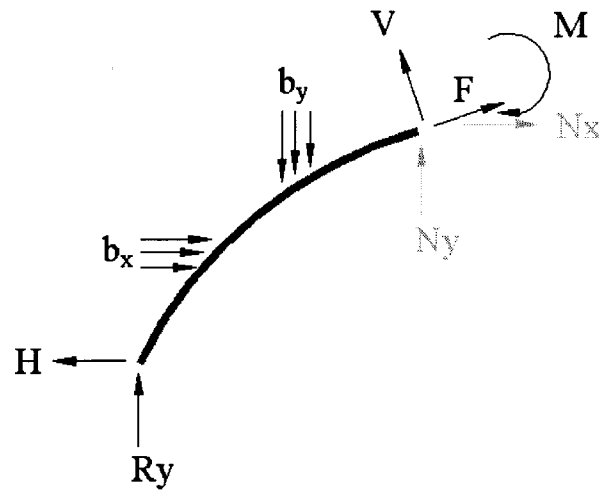


Figure 5: Equilibrium Force Equations for an Arch

$$N_x = F \sin \phi + V \cos \phi \quad \text{Eqn. 1}$$

$$N_y = F \cos \phi - V \sin \phi \quad \text{Eqn. 2}$$

$$\sum F_y = N_y - \int b_y dx + R_y \quad \text{Eqn. 3}$$

$$\sum F_x = N_x + \int b_x dx - H \quad \text{Eqn. 4}$$

$$\sum M = \int b_x x dx + \int b_y y dy - R_y x - H y \quad \text{Eqn. 5}$$

As seen from the equations 1 and 2, the shear and axial forces within an arch are coupled. As a consequence, under purely vertical load or purely horizontal load, both vertical and

horizontal reactions must be resisted at the foundation. This behavior is unlike typical beams; a beam loaded with purely vertical load only resists vertical reactions at the supports.

Although the arch equations allow for an arch to experience shear, bending, and axial stresses, an optimized arch will experience primarily axial compression under load. Specializing equation 5 for the case where no moments are allowed in the structure, and assuming the arch is not subjected to any horizontal loads, the following equation results.

$$y(x) = \frac{\int b_y x dx - R_{yx}}{H} \quad \text{Eqn. 6}$$

where $y(x)$ represents the required distance between the springing (or tension tie) to the centerline of the arch. The numerator in equation 6 is the exact expression for the moment in a simply supported beam; the denominator is the value of the horizontal reaction. From this equation, one can see that an optimized arch, i.e. one that experiences no bending, is a scaled version of the moment diagram of a simply supported beam subject to transverse loads.

In order for the optimized arch shape to be symmetrical, the applied loading must be symmetrical. To attain a symmetric and parabolic arch curve, the design load must be a uniformly applied vertical load loading throughout the arch. Fortunately, a series of equal point loads equally spaced will also yield a symmetric shape that is nearly parabolic; however, the resulting shape will not be a smooth curve. If the load on a parabolic arch is not symmetric, or if the load pattern does not conform to the bending diagram of the optimized shape, the arch will experience bending. The critical load pattern for an arch is the case where only half the span is loaded. Under this condition the maximum moment develops at the quarter point of the arch.

2.0 Funicular Method of Arch Design

For every load pattern on an arch, there exists an optimum arch shape, for which the applied loading is resisted through purely axial action. No bending stresses exist in the arch under this condition. There are several procedures used to determine the optimal arch shape. All these procedures are based on the same objective: no moment in the arch. For a given load configuration, there are an infinite number of optimal shapes. A particular solution is generated by specifying a constraint, such as the arch length, three pre-determined points along the arch, or the thrust force (Allen, 1998).

A funicular method of design, a graphical or numerical procedure, derived from equation 6, is used in this study to determine the optimum arch shape. The word *funicular* comes from the Latin word, funiculus, meaning “string.” (Allen, 1998) A funicular shape is the form a piece of string would take under an applied load. Similar to a string, a funicular shape resists load through axial action. A piece of string supporting uniform loads or equally spaced concentrated loads takes the form of a parabola. Thus, a parabola is the optimal shape for a structure resisting uniformly applied vertical loads through axial action. (Heller, 1963).

The procedure, specialized for the constraint of three pre-determined points that the arch must pass through, depends on the fact that the horizontal component of the force, N_x , at each section of the arch is constant. This horizontal force is also equal to the thrust at the foundation.

The first step in the funicular method is to determine the moment diagram (or distribution) along the arch due to all vertically applied loads, including the self-weight of the arch. The self-weight of the arch is typically not known during this first step. Thus, for the first design iteration, a self-weight distribution is assumed. The moments are

summed on a horizontal projection of the arch length. That is, the arch is assumed to be a simply supported beam. To determine the value of the constant horizontal force, N_x , the moment force at one constrained location is divided by the established distance between the arch centerline and the springing. The required distance from the arch centerline to the springing for every other point along the arch is found by dividing the moment at that particular section by N_x . (Allen, 1998)

3.0 Disadvantages of Traditional Arch Design

Further study into the funicular method and equation 6 identifies an important disadvantage of arch design: an arch shape is only optimal for a particular load pattern. If the distribution or magnitude of the loads are altered, the stresses along an arch change; thus the arch shape will need to be altered for optimal conditions. However, arches are static structures and it is unrealistic to change the structural geometry according to transient load patterns. Consequently, traditional arch design utilizes the dominant load configuration to determine the arch shape. For arch bridges, the dominant load (the design load combination) is an arch loaded with full dead load and half the design live load. For most other arches, the dominant load is an arch loaded with full dead load. Under these conditions an arch will have purely axial action. It is usually under other load cases, particularly live load that arches experience bending.

Depending on the arch structure, the bending due to secondary load cases may be significant. The need to design an arch to resist bending in addition to axial loads diminishes the attractiveness of arch structures. A more efficient arch design incorporates a mechanism to limit the bending stresses in the arch to a pre-defined allowable limit. Active controls applied to an arch provides an example of how efficiency of a structure improves with the application of external control devices.

4.0 Active Control

A significant amount of inefficiency in structural systems results from the need to design a structure for all possible design load conditions. Further, this type of structural design is contingent upon always having reliable knowledge of the relative magnitude of all loads the structure that will be applied to the structure (Connor, 1999).

The introduction of passive mechanisms of control has increased the efficiency of structures by preventing loads from entering a structure, as in the case of base isolators used to isolate a structure from seismic ground accelerations. Damping systems are also utilized to dissipate the amount of energy, and therefore, stresses and movement the structure experiences from dynamic loads. The shortcoming of these systems is that they too are dependent on reliable knowledge of expected forces the structure will experience. Both these devices are designed according to expected forces. (Connor, 1999)

The benefit of active controls is that they can accommodate unexpected loads imposed on a structure. Active control devices are designed to monitor structural variables, such as forces and displacements the structure is experiencing. The mechanism then determines if the displacement or force exceeds pre-defined limits. In this case, the system determines a set of actions that will change the structural state to an acceptable one. An actuator, a mechanical device, induces a force or displacement according to the determined actions to counteract externally applied forces or displacements (Connor, 1999).

4.1 Components of Active Control System

Active control devices are composed of three main components: the monitor, the controller, and the actuator. The monitor is a set of sensors located along the structure used to monitor structural variables discussed above. The controller is a cognitive module, in some cases, with adaptive learning, which analyzes the sensor readings and

uses a control algorithm to determine what actions to take to limit the forces or displacements. The actuator implements decisions made by the controller. All the components depend on an external energy source to investigate and implement decisions. Figure 6 demonstrates the relationship and interaction between the components of an active control system. (Connor, 1999)

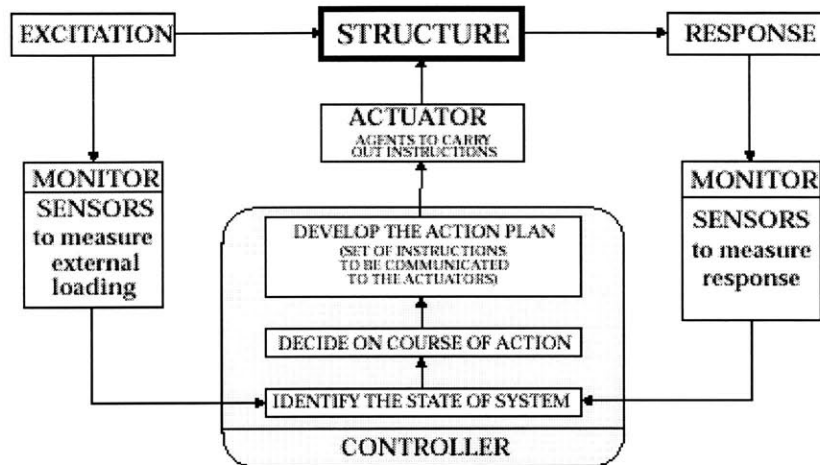


Figure 6: Components of an Active Control System

Since force actuators require time to apply the force, the controller must have the capability to predict forces a short distance off from the actuator. In the case of a bridge, this scheme can be implemented if the controller was able to compute the weight and velocity of a load moving along the deck. With this known information, the controller can predict the impact of the load on the structure and send a signal to the actuator to apply a counteracting force to maintain the forces in the arch to a prescribed limit. (Connor, 1999)

Current technology is able to support the sensors and algorithms required for the controllers. However, actuator technology requires further advancement before active control technology can be applied to large civil structures. Civil structures generally require actuators to deliver large force to a system and to have short response times (generally on the order of a few milliseconds). There are a number of different types of

actuators that can impose a large force on a system; however, these actuators have long response times. Most actuators require a large amount of energy to deliver the required forces. Before active control technology can be implemented in civil structures, actuators that are capable of delivering thousands of Newtons of force to a system within a few milliseconds without requiring a large amount of external energy must be developed. Alternately, the cost and ease of installing the system must improve so that multiple actuators can be installed in a structure. (Connor, 1999)

4.2 Actuator Technology

There are three types of actuators technologies: hydraulic, electro-mechanical, and electro-magnetic linear actuators. Each type of actuator has two components, a piston and a gear mechanism. The gear mechanism applies a force to the piston in order to translate the piston. Consequently, the piston applies a force to the structure and a reaction force is felt by the gear mechanism. In cases where there is not adjacent surface to absorb the reaction from gear mechanism, a self-equilibrating actuator system is utilized. (Connor, 1999)

An ideal actuator system is one that can deliver a large amount of force in a small duration of time using minimal external energy. To control moment distributions on a structure linear actuators must be placed below or above a structure. One self-equilibrating actuator scheme, applicable to the arch structure, is composed of three rods and a gear mechanism (see Figure 7). (Connor, 1999)

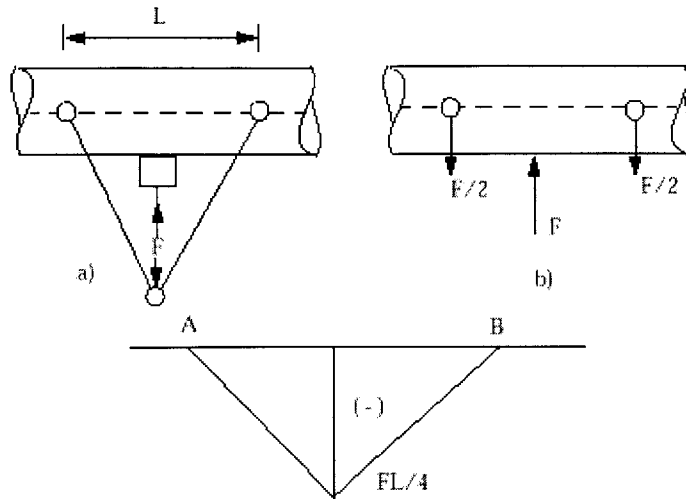


Figure 7: Three-rod Actuator scheme

The vertically applied load F is equilibrated by vertical component of the force in the diagonal rods. The forces cause a triangular moment field. A compressive force, of magnitude $F/2$ is induced in the localized area. The shear force in the localized area is also expected to increase. With a number of these actuator-rod configurations placed in series, one can generate a piece-wise linear bending moment distribution.

4.3 Active Control Algorithm

The first step of determining the active control algorithm is to set a pre-defined limit on the allowable stresses the system can withstand. For the case where moments need to be controlled it is necessary to specify the maximum allowable moment, $M(x)^*$.

The moment a structure feels at any point in time is the sum of the moment due to dead, live, or other loads, M_d , and the moment caused by the active control, M_c .

$$M^* \geq M(x) \equiv M_d(x) + M_c(x) \quad \text{Eqn. 7}$$

The design objective is to limit $M(x)$, the moment at any point in the structure, to $M(x)^*$:
Using matrix notation, this simplifies equation (7) to the following:

$$-M_d - M^* \leq M_c \leq M^* - M_d \quad \text{Eqn. 8}$$

From the range of acceptable control moments, M_c , one generates the target distribution, M_c^* . The sensor on an active control system senses the forces or moments at specified locations on the structure. If the number of actuators on the system (r) is equal to the number of sensor locations (n), the algorithm for the active control simplifies to applying the actuator load to induce M_c^* at the sensor location. In this case, M_c^* will always be equal to M_c . In most cases, the number of sensors on the system exceeds the number of actuators ($n > r$). In this case, it is not possible to obtain the exact value of M_c^* at every sensor location. In this case, M_c is a linear combination of moments caused by several actuators. (Connor, 1999)

$$M_c = \Psi m \quad \text{Eqn. 9}$$

The error between M_c^* and M_c is designated by e :

$$e = M_c^* - M_c = M_c^* - \Psi m \quad \text{Eqn. 10}$$

ψ is a vector of size $n \times r$, which represents the distribution of moments due to a single actuator; m represents the maximum magnitude of the moment field. In the case, where the number of sensor exceeds the number of actuators, the goal of the control algorithm is to minimize e using a least square algorithm. The least square method can be used to determine an appropriate solution for $e = 0$. The error measure is taken as the norm of J (Connor, 1999):

$$J = \frac{1}{2} e^T e \quad \text{Eqn. 11}$$

Requiring \mathbf{J} to be stationary with respect to each moment parameter contained in m leads to a simple matrix equation

$$\frac{\partial J}{\partial m} \Rightarrow am = b \quad \text{Eqn. 12}$$

where,

$$a = \Psi^T \Psi \quad \text{Eqn. 13}$$

$$b = \Psi^T M_c^* \quad \text{Eqn. 14}$$

5.0 Active-Controlled Arch Structure

Active control implemented on an arch structure is an ideal application of the technology. With active controls, the arch shape and sections can be designed to carry the dominant design load pattern through axial behavior. Rather than designing the arch to resist stresses, particularly those produced by bending, caused by additional load cases, other load cases will be supported by adjustments made by the active control mechanism. The benefit of this system is an arch structure that primarily carries axial load and a minimal amount of bending, regardless of the load configuration.

6.0 Design of Proposed Charles River Crossing Bridge Arch

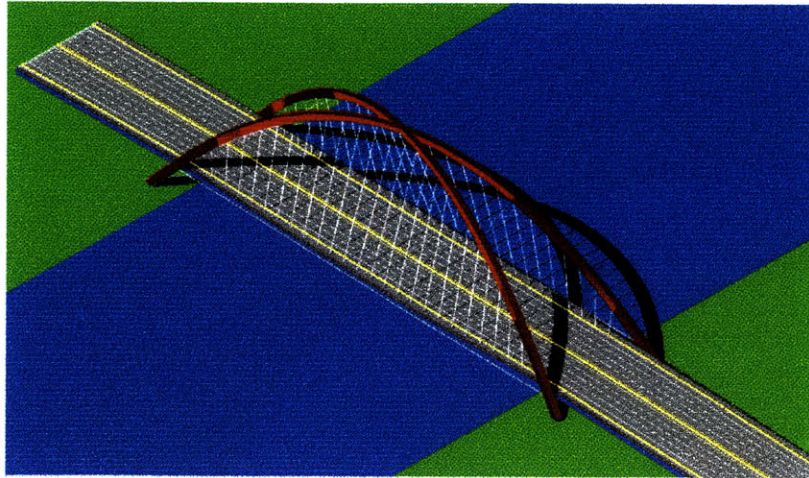


Figure 8: Proposed Charles River Crossing Bridge

6.1 Introduction

Components of the applicable design conditions and criteria of the proposed Charles River Crossing Bridge (see Figure 8) will be utilized in this study. Active Control theory will be implemented in the design procedure to demonstrate the reduction in bending stresses in the arch under critical load conditions. The proposed bridge, a 750-foot span, segmental, pre-cast concrete, two-hinge arch bridge is seen on Figure 8. The rise of the proposed bridge is 250 feet from the waterline. A unique feature of this bridge is the location of the tie. Typically, the tie on an arch is located at the foundation level. Since the bridge spans over a water crossing, the tie had to be placed at higher elevation. Currently, the tie is at deck level and braced by the deck superstructure. The arch is constructed of concrete box sections, which taper in depth from the crown of the arch to the base. Loads are imposed on the arch through a series of suspension cables. For the design, a two-dimensional model of one of the arches is idealized. For purposes of demonstrating the use of active controls to minimize bending in the arch, the out of plane forces caused by the inclined cables are neglected.

The design of the arch is a two step procedure. The first phase involves determining the optimal shape of the arch for the dominant design load. Further, the arch must be checked to ensure it provides adequate axial capacity for all load combinations. The second phase of the design is the implementation of the active control system.

The design load combination for an arch is full dead load and half the live load. The dead weight is typically significant portion of the dead weight. The arch cross-section is optimized for the required stress capacity for the design load combination. The iterative nature of arch design is a result of changes in the arch self-weight as the arch cross-section and shape is revised. The basic design procedure utilized in this case to determine the optimum arch shape is outlined in the following steps.

1. Determine imposed loads on the arch, specifically imposed dead and live loads.
2. Specify geometric constraints, specifically three pre-defined points.
3. Determine funicular shape of arch for dead and live loads from superstructure.
4. From estimated value of axial force near crown, establish required section properties required at arch crown.
5. Using coordinates found from funicular method, perform regression analysis to determine fourth-degree polynomial of arch shape
6. Estimate weight of arch per linear foot (utilizing derivative of polynomial)
7. Determine funicular shape for dominant load case.
8. Verify adequacy of sections for design axial forces for all load combinations.
9. Iterate section properties, as necessary
10. Return to step 4, as necessary.

6.2 Loads

There are two distinct types of loads imposed on an arch: loads from the superstructure and the self-weight of the arch. Superstructure loads include design dead and live loads on the superstructure. The superstructure loads are transmitted to the arch through the cables.

6.2.1 Superstructure Loads

Table 1 lists the imposed dead and live loads from the bridge superstructure. The ID number listed on Table 1 corresponds to points found on Figure 9. Typically each cable is spaced at 25.8 feet along the arch axis. Under the dominant design load pattern each cable carries approximately 280 kips of load. From Table 1 one can see the loads in the cables change at the extreme ends of the arch. Geometric compatibility between the arch, the deck, and required pedestrians access forced the re-alignment of the cables at these locations. Consequently, cables at the ends have a greater tributary area of load to carry.

Table 1: Imposed Design Dead and Live Loads

ID	x-Distance	Cable Dead Load	50% Cable Live Load	Total Imposed Load
	feet	kips	kips	kips
	0.0			
3	45.8	399	42.69	441
4	71.5	148	51.54	199
5	97.2	243	49.59	293
6	122.9	220	50.11	270
7	148.6	228	50	278
8	174.3	228	50	278
9	200.0	229	50	279
10	225.7	230	50	280
11	251.4	231	50	281
12	277.2	232	50	282
13	302.9	232	50	282
14	328.6	232	50	282
15	354.3	233	50	283
16	367.2			
17	380.0	233	50	283
18	405.7	232	50	282
19	431.4	232	50	282
20	457.1	232	50	282
21	482.8	231	50	281
22	508.6	230	50	280
23	534.3	229	50	279
24	560.0	228	50	278
25	585.7	227	50	277
26	611.4	224	50	274
27	637.1	227	50	277
28	662.8	210	50	260
29	688.5	260	50	310
	716.3			

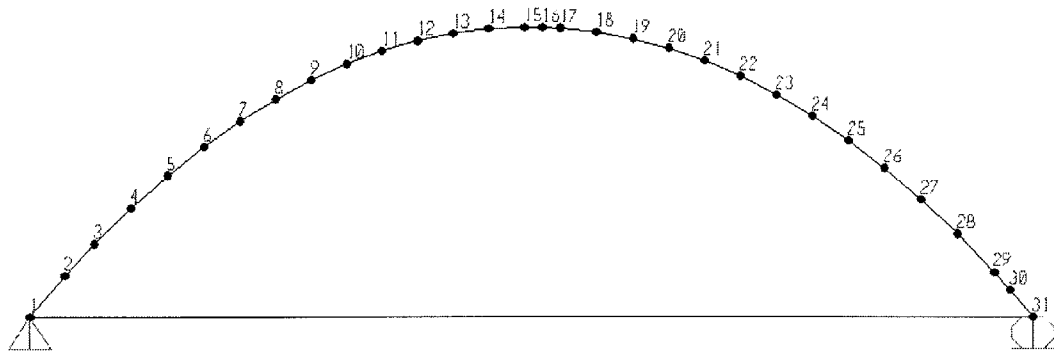


Figure 9: SAP2000 Model of Arch

6.2.2 Self-weight

The arch was designed to taper in depth from a square box section at the crown to rectangular box section at the base. The taper is implemented for structural reasons: the compressive stresses in the arch increase towards the supports. The taper allows for the area of the section to increase in proportion to the increase in axial stresses. The variation in depth and the calculation of the arch self-weight was formulated according to Melan's method of arch design. The method approximates the change in depth, d , according to the secant of the enclosed angle (Melan, 1915):

$$d = d_o \sec \phi \quad \text{Eqn. 15}$$

$d_o = \text{depth of arch at crown}$

$\phi = \text{enclosed angle}$

Accordingly, the self-weight, q , of the arch is expressed as:

$$q = d \gamma w \sec \phi, \quad \text{Eqn. 16}$$

$$\text{or } q = w d_o \gamma (1 + \tan^2 \phi) \quad \text{Eqn. 17}$$

$w = \text{width of arch}$

$\gamma = \text{unit weight of concrete}$

150 pcf

6.3 Funicular method

The funicular method as described in Section 2.0 is used in this study to determine the optimal arch shape. Specifically, the numerical version of the procedure specialized for the case where three pre-defined points along the arch are known is utilized.

6.3.1 Determination of Constraints

As discussed earlier, the deck braces the tension tie of the arch. The deck in turn must connect to existing viaducts on either end of the bridge. These geometric constraints dictated the location of 2 of the three pre-defined points required for the funicular method. The arch must intersect with the deck at the end of the deck at both ends. The third required point was determined by the desired maximum height of the arch, 250 feet, above the waterline. Figure 10 describes each of these points.

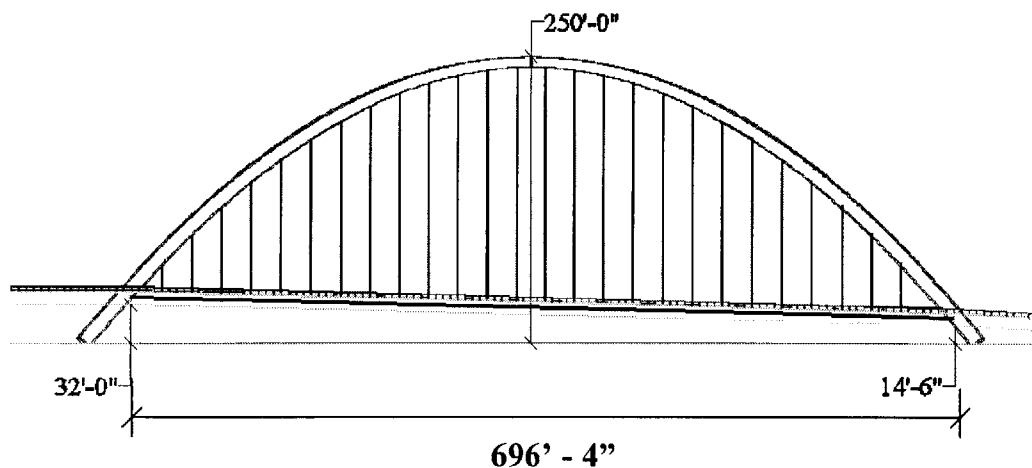


Figure 10: Required Geometric Dimensions for Arch

6.3.2 Determination of optimal arch shape

The first iteration of the design was the determination of the funicular arch shape from only the applied superstructure loads using the method described in Section 2.0. A regression analysis was performed on the resulting coordinates to determine a fourth degree polynomial, $h(x)$, describing the arch shape. The polynomial was necessary to approximate the tangent of the enclosed angle with the first derivative of the arch shape:

$$\tan \phi \approx \frac{d}{dx} h(x)$$

The first iteration through the funicular method revealed an approximate value of the axial force in the arch near the crown. Since the first iteration was performed using only the superstructure loads, the computed axial force was significantly less than an iteration including the self-weight of the arch. The initial value for the arch cross-section was determined by assuming the required axial capacity of the arch at the crown was double the value of the axial force found from this first iteration.

All further iterations of the funicular method utilized the dominant load case, full dead load plus half the design load, to determine the optimal arch shape. The calculations for the funicular arch shape are found in Appendix 1. The values in the chart are from the final iteration. The procedure utilized is as described in Section 2.0.

6.4 Computer Model

After a couple of iterations through the funicular method, a model of the arch was constructed in SAP2000. Figure 9 depicts the SAP2000 model. Since SAP2000 is not able to idealize a tapered member, sections of the arch were discretized. The depth of each discretized section was found by maintaining the weight of each section. The weight

of each segment was found using the eqn 16, which describes the weight per linear foot of the arch. Appendix 2 contains a spreadsheet of the calculated discretized depths. SAP2000 was used in conjunction with interaction diagrams (see Appendix 4) to ensure the axial capacity of the arch was sufficient to resist loads resulting from the governing load cases. Following are the three governing load cases:

Load Combination 1 (design load pattern): Dead Load plus half the Live Load over the entire arch.

Load Combination 2: Dead Load plus the entire Live Load over the entire arch.

Load Combination 3 (critical load pattern): The arch loaded with full Dead Load, but only half the arch loaded with Live Load.

In total, four iterations were performed until convergence of the stresses and the coordinates was observed.

6.5 Optimized Arch Shape

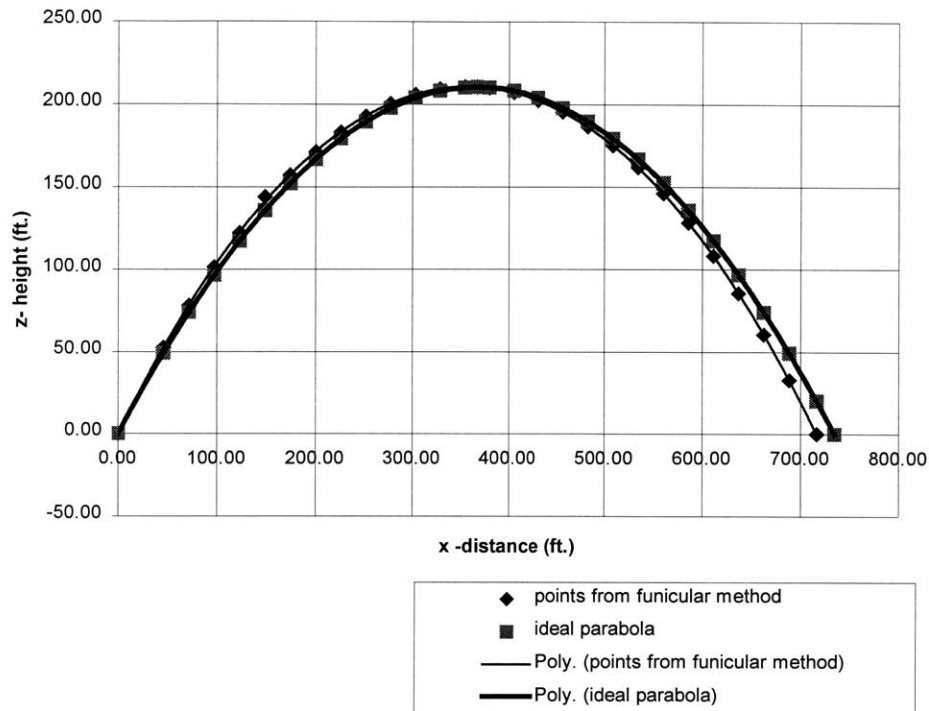


Figure 11: Optimized Arch Shape

A graph of the final arch shape is found on Figure 11. Also shown is a graph of an idealized parabolic shape of the arch found using the pre-defined geometric points. As shown, the points do not differ significantly, but the small variation eliminates bending from the arch. The base of the arch shown in Figure 11 is actually the intersection of the arch with the deck. During the design, it was realized that continuing the arch curve to the foundation level induced major bending in the arch. The additional bending force is proportionate to the vertical reaction at the deck level and the horizontal eccentricity between the arch at the deck level and the foundation. Eliminating this eccentricity completely eliminates the additional bending stress. Thus, to minimize the amount of bending in the arch, the arch curvature should discontinue at the tie level. Instead, vertical supports should extend from the arch at the deck level to the foundation.

6.6 Discussion of Design Stresses

The last load combination is the critical load combination for arches since the non-symmetrical loading maximizes the bending stresses in the arch, as seen from Figures 12 and 13. The bending stresses in the arch under Load Combination one are negligible (Figure 12). The moments observed in the arch under Load Combination one is due to the discretized sections. The moments in the arch under Load Combination three are significant (Figure 13). The moment is maximized at the quarter point where the moment is approximately 16,800 kip-ft. With traditional arch design, the arch cross-sections are designed to resist these moments.

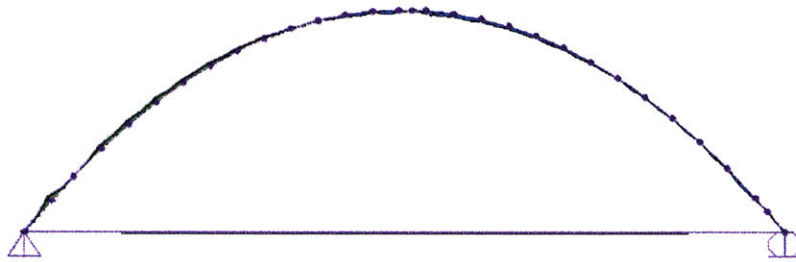


Figure 12: Moment Diagram of Arch under Design Load Combination (1)

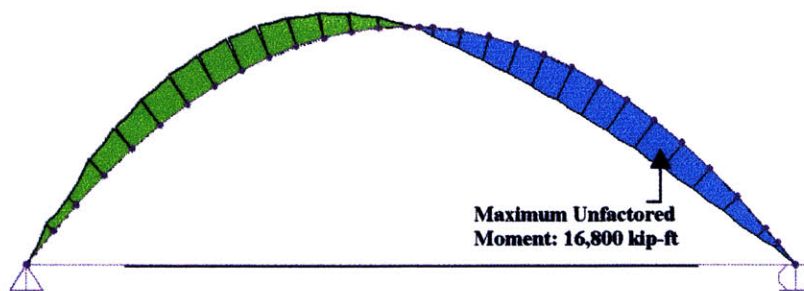


Figure 13: Moment Diagram of Arch under Critical Load Combination (3)

The interaction diagram for the section where the moment is maximized is shown in Figure 14. At this location, the section is approximately 9.5 ft. deep. The section is designed to have adequate axial capacity for all governing load combinations. However, as traditional design would suggest, the section was not designed for moment capacity for

all load combinations. As the interaction diagram in Figure 14 demonstrates, the section located at the point of maximum moment does not have sufficient moment capacity to resist the force under the critical load combination. The use of active control on the arch structure eliminates the need to design sections for critical moment stresses.

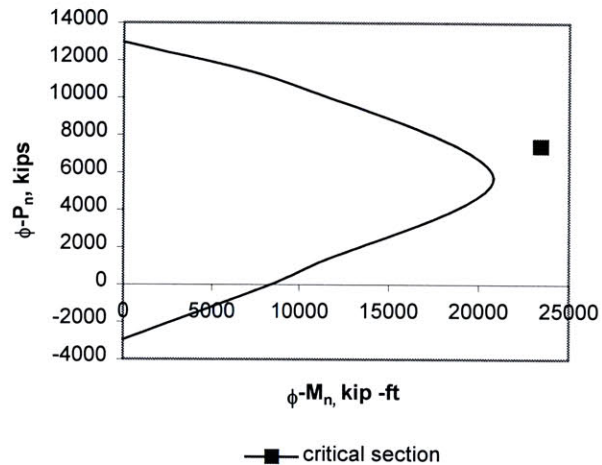


Figure 14: Interaction Diagram for Critical Section

7.0 Design of Active Control System

The objective of the active controls in the arch is to limit the moments in the arch to a pre-defined limit. The three-rod actuator scheme discussed in Section 4.2 is used on the arch to control moments. The benefit of this actuator scheme is that the forces and moments generated in the arch are restricted to a localized area. Further, the stresses induced by a particular actuator are equilibrated within the restricted length.

7.1 Configuration of Actuators

The actuators are placed in series along the arch in order to generate a piece-wise linear moment field. The actuator configuration is as shown in Figure 15.

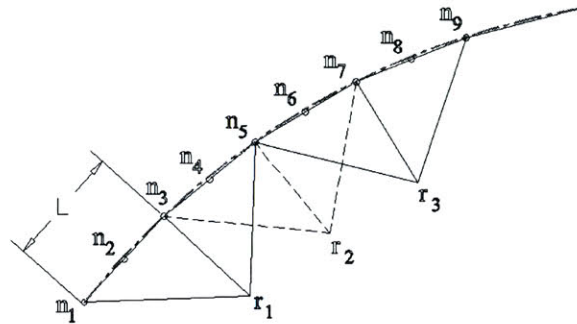


Figure 15: Proposed Actuator Scheme on Arch

For purposes of implementing the actuator scheme, the arch was idealized by a series of twenty feet long beams placed in series. Moments are monitored along the arch at the start, midpoint, and end of each beam segment. The locations where moments are monitored are designated by n_i (Refer to Figure 15). The piston corresponding to each actuator is placed at the intersection of every beam segment. The location of an actuator is designated in Figure 15 by r_i . The moment field produced by each actuator is distributed over the lengths of two beams segments. The actuators are placed normal to the intrados (interior) of the arch. Since each moment field is restricted to a relatively short length of the arch, the length over which the moment field is applied can be approximated to be linear. Consequently, traditional beam theory can be used to determine resulting shear, axial and moments over the localized length.

7.2 Active Control Algorithm

In order to demonstrate the effect of active control on an arch, M^* , the limiting moment capacity, was a constant value for all areas along the arch. Since the arch tapers, a more realistic, and more complex, algorithm would include varying M^* along the length of the arch. The value of M^* at each point would be selected according to the bending capacity of the arch section and the axial load the section is experiencing. For this study, M^* was selected to be 6000 kip-ft. This value is slightly less than the maximum allowable stress in the arch crown with the current axial stress in the arch.

A Matlab program was formulated to compute the actuator forces required to limit the moments throughout the arch to M^* . A copy of the Matlab input is seen in Appendix 3. The Matlab algorithm was designed to find the appropriate control moments when the arch is under the critical load pattern.

7.3 Results of Active Control Algorithm

Below are the results from the Matlab algorithm. Figure 16 demonstrates the applied loading, M_d , the range of acceptable control moments, M_{c-} and M_{c+} , and the target control moment, M_{c^*} .

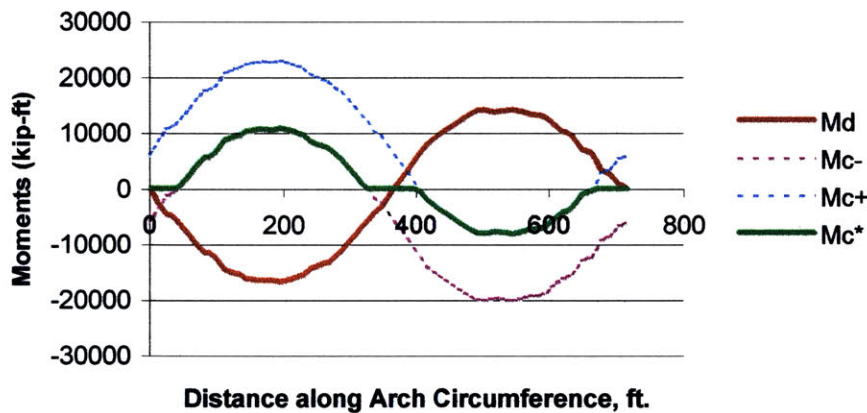


Figure 16: Graph of Critical Design Moments (M_d) and Target Control Moment Distributions (M_{c^*})

The area between the dotted curves of M_{c-} and M_{c+} represent the range of acceptable control moments. The target moment field, M_{c^*} , was selected based on minimizing the required control moment to bring the arch within the acceptable range of bending stresses. Figure 17 depicts the target control moment and the resultant control moments found from Matlab. Also included is e , the summation of the design moments and the control moments. As seen in the Figure, the resultant control moments, M_c , are very

close to the target moment field, M_c^* . The graph of e demonstrates that maximum moment along the arch is approximately 6000 kip-ft. This was the expected result.

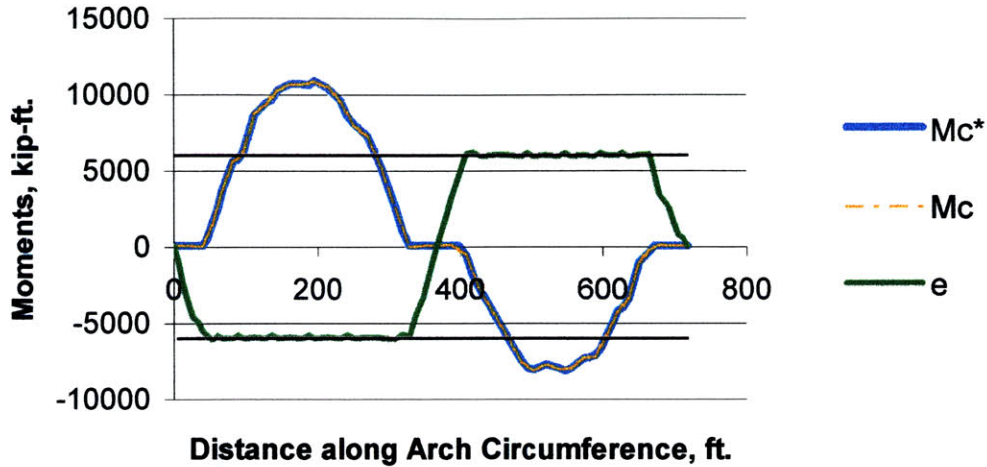


Figure 17: Graph of resulting Control Moments (M_c) and sum of moments on structure (e)

The actuator force required to deliver the peak control moment, which coincides with the location of the critical section described above, is 2200 kips. Using the same interaction diagram created above, the stresses at the critical section are compared before and after the implementation of the active control system (see Figure 18)

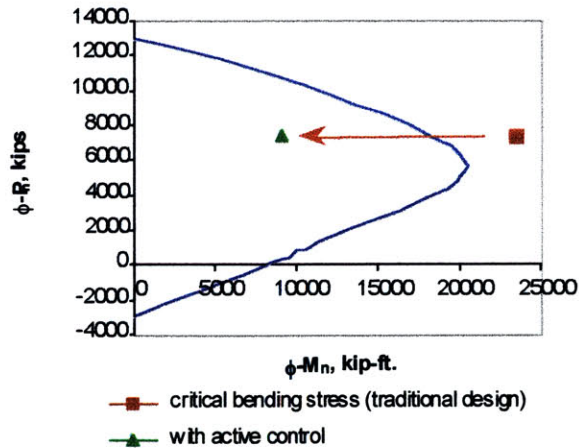


Figure 18: Interaction Diagram of Critical Section of Arch

As the interaction graph demonstrates, the section is now sufficient to resist required stresses even at the critical loading. The moment in the section decreased by 54%.

8.0 Conclusion

Arches have been used for centuries in structural engineering. The continuing use of arches is due to the efficiency of the system and the aesthetic appeal of the structure. Arch structures resist load primarily through axial action. The weakness of an arch is it may develop considerable bending stresses when subject to non-uniform or random load patterns. The use of active controls in an arch successfully decrease the bending stresses in an arch to a pre-scribed limit. The result is an arch structure, which resists all load patterns primarily through axial action. Consequently, the construction material is utilized very efficiently.

This result is not without consequence or cost. The actuator requires external energy. The cost of material, labor and construction of the traditional method must balance the cost of the actuator scheme, including the physical components and the energy source. A broader analysis should also incorporate long term savings of implementation of the actuator as a means to take care of future load requirements, the aesthetic appeal of a less bulky structure, the cost of maintaining the system, and the tested reliability of such a system.

Currently, an analysis of the system with current technology would probably suggest the traditional design. In the future, when the technology able to support such a system at a economical cost is available and scientific and public trust in such a system has been established, the use of active controls to build more reliable, intelligent, civil systems will be a viable alternative.

APPENDIX 1

Typical cable spacing 25.716

ID	x-Distance	Cable Dead Load	50% Cable Live Load	Total Imposed Load
	feet	kips	kips	LOAD
1	0.0			
2	45.8	399	42.69	441
3	71.5	148	51.54	199
4	97.2	243	49.59	293
5	122.9	220	50.11	270
6	148.6	228	50	278
7	174.3	228	50	278
8	200.0	229	50	279
9	225.7	230	50	280
10	251.4	231	50	281
11	277.2	232	50	282
12	302.9	232	50	282
13	328.6	232	50	282
14	354.3	233	50	283
15	367.2			
16	380.0	233	50	283
17	405.7	232	50	282
18	431.4	232	50	282
19	457.1	232	50	282
20	482.8	231	50	281
21	508.6	230	50	280
22	534.3	229	50	279
23	560.0	228	50	278
24	585.7	227	50	277
25	611.4	224	50	274
26	637.1	227	50	277
27	662.8	210	50	260
28	688.5	260	50	310
29	716.3			

APPENDIX 1

Z -height at center
Horizontal Force

210.5 ft. from base
4823.757 kips

COORDINATES FOUND FROM
FUNICULAR METHOD

RESULTING FOURTH DEGREE POLYNOMIAL
 $y = -7.654E-10x^4 + 1.106E-06x^3 - 2.145E-03x^2 + 1.250E+00x - 1.543E-01$

x	y
0.00	0.00
45.76	52.64
71.47	78.18
97.19	101.58
122.90	122.46
148.61	144.20
174.32	157.28
200.03	171.32
225.74	183.17
251.45	192.87
277.16	200.46
302.87	205.96
328.58	209.37
354.29	210.73
367.22	210.50
380.00	210.02
405.71	207.25
431.42	202.40
457.13	195.47
482.84	186.42
508.55	175.23
534.26	161.87
559.97	146.28
585.68	128.43
611.39	108.24
637.10	85.64
662.81	60.54
688.52	32.91
716.27	0.00

x	z
0.00	0.00
25	29.77
45.76	52.66
71.47	78.62
97.19	102.01
122.90	122.95
148.61	141.49
174.32	157.71
200.03	171.68
225.74	183.45
251.45	193.06
277.16	200.55
302.87	205.96
328.58	209.30
354.29	210.59
367.22	210.47
380.00	209.84
405.71	207.04
431.42	202.18
457.13	195.25
482.84	186.22
508.55	175.06
534.26	161.72
559.97	146.15
585.68	128.30
611.39	108.10
637.10	85.48
662.81	60.35
688.52	32.62
700	19.38
716.27	-0.32

APPENDIX 2

Section ID	Length ft	Weight kips	d ft.
1	38.9	246.2	11.1
2	30.9	186.3	10.4
3	36.5	210.3	9.8
4	34.8	190.5	9.2
5	33.2	173.3	8.6
6	31.7	158.4	8.1
7	30.4	145.7	7.7
8	29.3	135.0	7.3
9	28.3	126.0	6.9
10	27.4	118.8	6.6
11	26.8	113.1	6.4
12	26.3	108.8	6.2
13	25.9	105.9	6.1
14	25.7	104.4	6.0
15	12.9	52.4	6.0
16	12.8	51.9	6.0
17	25.9	105.4	6.1
18	26.2	107.9	6.2
19	26.6	111.8	6.3
20	27.3	117.1	6.5
21	28.0	123.9	6.8
22	29.0	132.3	7.1
23	30.1	142.4	7.5
24	31.3	154.5	8.0
25	32.7	168.6	8.5
26	34.2	184.9	9.0
27	36.0	203.7	9.6
28	37.8	225.3	10.2
29	17.5	108.3	10.7
30	25.6	162.5	11.1

q = weight per linear foot

$$q = -.522E-17x^7 + .132E-13x^6 - .294E-10x^5 + .358E-7x^4 - 3.56E-5x^3 + .0216x^2 - 10.368x$$

Depth Calculation for Discretized SAP Model

$$W = L * A * \gamma$$

$$W = L * (6d_n - 3(d_n - 3)) * \gamma$$

L = length of section

γ = unit weight of concrete

A = Area of section
= $6d_n - 3(d_n - 3)$

d_n = depth of section

$$d_n = \frac{W - 9L\gamma}{3L\gamma}$$

Total Weight **4275.6**

```

clear
diary thesisfinal.diary
hold on
%Units are kip, feet

% ARCH COORDINATES (x,y);
% X contains a list of observed points(n)
X=wklread('xvalues');
% p is the fourth degree polynomial representing the arch curve
p =[-7.654e-10 1.106e-6 -2.145e-3 1.25 -1.543e-1] ;
% TO DETERMINE Y COORDINATES, EVALUATE THE POLYNOMIAL AT X
Y = polyval(p,X);

% PLOT ARCH COORDINATES
%plot(X,Y);

% Determine length of arch segments (all segments should be 20 ft. in
length)
for n=1:2:(length(X)-1)
for i=1:((length(X)-1)/2)
L(i)=sqrt((X(n+2)-X(n)).^2+(Y(n+2)-Y(n)).^2);
end
end
L

% Md is a vector of the moments the arch is experiencing under the
critical load

Md=wklread('moments')

% Mstar is a vector of the allowable moments
Mstar = 6000;

%Determine range of Mc, the control Moment
for j=1:length(Md)
Mcl(j)=Mstar-Md(j);
end;
Mcl=Mcl'
```

```

for j=1:length(Md)
    Mc2(j)=-Mstar-Md(j);
end;

Mc2=Mc2'

%Determine the target, optimal control moment

for j=1:length(Mc1)
    if Mc1(j)>0
        if Mc2(j)>0;
            Mt(j)=Mc2(j);
        end;
    end;
    if Mc1(j)<0;
        if Mc2(j)<0;
            Mt(j)=Mc1(j);
        end;
    end;
    if Mc1(j)>0;
        if Mc2(j)<0;
            Mt(j)=0;
        end
    end
    if Mc1(j)<0;
        if Mc2(j)>0;
            Mt(j)=0;
        end
    end
end;

Mt=Mt'

% TYPICAL PSI FUNCTION

TYP = [0 .75 1 .75 0]'

psi=zeros(2*length(L)+1,length(L)-1);

for i=1:length(L)-1
    psi((2*i-1):(2*i+3),i:i)=TYP(1:5,1:1);
end;
psi;

%The solution to the unknown moments is aM=b, where M=inverse(a)*b
a=psi'*psi;

b=psi'*(Mt);

M=inverse(a)*b

Mc=psi*M

e=Md+Mc

for i=1:length(e)

```

```
if e(i)>0
error(i)=e(i)-Mstar;
else
error(i)=e(i)+Mstar;
end;
end;
```

```
error=error'
```

```
plot(X,Md,'y')
plot(X,Mc1,'m')
plot(X,Mc2)
plot(X,Mt,'r')
%plot(X,M,'g')
plot(X,e,'b')
plot(X,Mc,'k')
%plot(X,error,'m')
```

```
wklwrite('outputx',X)
wklwrite('outputmc1',Mc1)
wklwrite('outputmc2',Mc2)
wklwrite('outputmt',Mt)
wklwrite('outputmd',Md)
wklwrite('outputmc',Mc)
wklwrite('outpute',e)
```

APPENDIX 4

MATERIAL PROPERTIES

f_c	4500 psi
f_y	60 ksi

SECTION TYPES

Section	<u>6 x 6</u>	<u>6 x 9.5</u>	<u>6 x 11</u>
height	72 in	90 in	132 in
base	72 in	72 in	72 in
tw	18.00 in	18.00 in	18.00 in
tf	18.00 in	18.00 in	18.00 in

SECTION PROPERTIES

Section	<u>6 x 6</u>	<u>6 x 9.5</u>	<u>6 x 11</u>
I_{xx}	101 ft⁴	188 ft⁴	538 ft⁴
I_{yy}	101 ft⁴	125 ft⁴	180 ft⁴
S_{xx}	17 ft ³	25 ft ³	49 ft ³
S_{yy}	17 ft ³	21 ft ³	30 ft ³
A_{sx}	18 ft ²	23 ft ²	33 ft ²
A_{sy}	18 ft ²	18 ft ²	18 ft ²
A_g	27 ft ²	32 ft ²	42 ft ²

APPENDIX 4

REINFORCEMENT

Section	<u>6 x 6</u>	<u>6 x 9.5</u>	<u>6 x 11</u>
<u>Layer 1</u>			
Bar #	9	9	10
No. of Bars	15	15	15
Steel Area1	14.91 in ²	14.91 in ²	18.41 in ²
Depth1	67 in	85 in	127 in
<u>Layer 2</u>			
Bar #	9	9	10
No. of Bars	10	15	10
Steel Area2	9.94 in ²	14.91 in ²	12.27 in ²
Depth2	62 in	80 in	122 in
<u>Layer 3</u>			
Bar #	9	9	10
No. of Bars	15	15	15
Steel Area3	14.91 in ²	14.91 in ²	18.41 in ²
Depth3	5 in	5 in	5 in
<u>Layer 4</u>			
Bar #	9	9	10
No. of Bars	0	10	10
Steel Area4	0 in ²	9.940195505 in ²	12.2718463 in ²
Depth4	10 in	10 in	10 in
ρ	1.02%	1.21%	1.01%
ρ_{min}	0.34%	0.32%	0.32%
ρ_{max}			

MOMENT CAPACITY CALCULATIONS (ref. ACI 10.2.7)

Balanced Moment

β	0.825
ϵ_u	0.003
f_y	60 ksi
E	29000 ksi
ϵ_y	0.002069
ϕ (bend.)	0.7

Section	<u>6 x 6</u>	<u>6 x 9.5</u>	<u>6 x 11</u>
c(bal)	39.65 in	50.31 in	75.16 in
a	32.71 in	41.50 in	62.01 in
.85*f_c	3825.00 psi	3825.00 psi	3825.00 psi
C_c	-6983 k	-8194 k	-11017 k
R_c	16.45	20.90	32.06
M_c	-162059 k-in	-240968 k-in	-474890 k-in
ϵ_1	0.00207	0.00207	0.00207
σ_1	60.0	60.0	60.0
T₁	895 k	895 k	1104 k
M₁	24465 k-in	31038 k-in	57252 k-in
ϵ_2	0.0017	0.0018	0.0019
σ_2	49.0	51.4	54.2
T₂	487 k	766 k	665 k
M₂	10891 k-in	30893 k-in	54784 k-in
ϵ_3	-0.0026	-0.0027	-0.0028
σ_3	-60.0	-60.0	-60.0
T₃	-895 k	-895 k	-1104 k
M₃	-31001 k-in	-31001 k-in	-38273 k-in
ϵ_4	-0.0022	-0.0024	-0.0026
σ_4	-60.0	-60.0	-60.0
T₄	0 k	-596 k	-736 k
M₄	0 k-in	-17685 k-in	-21834 k-in
phi	0.70	0.70	0.70
N	-6496 k	-8024 k	-11088 k
	-4547 k	-5617 k	-7762 k
M_n	19035 k-ft	29299 k-ft	53919 k-ft
ϕ-M_n	13324 k-ft	20509 k-ft	37744 k-ft

APPENDIX 4

Pont 1

Section	<u>6 x 6</u>	<u>6 x 9.5</u>	<u>6 x 11</u>
c₁	72.00 in	90.00 in	132.00 in
a	59.40 in	74.25 in	108.90 in
.85*f_c	3825.00 psi	3825.00 psi	3825.00 psi
Cc	-11402 k	-13013 k	-16772 k
Rc	29.70	37.13	54.45
Mc	-338626.3 k-in	-483094.6 k-in	-913227.8 k-in
ε₁	-0.0002	-0.0002	-0.0001
σ₁	-6.0	-4.8	-3.3
T1	-90 k	-72 k	-61 k
M1	-450 k-in	-360 k-in	-303 k-in
ε₂	-0.0004	-0.0003	-0.0002
σ₂	-12.1	-9.7	-6.6
T2	-120 k	-144 k	-81 k
M2	-1201 k-in	-1441 k-in	-809 k-in
ε₃	-0.0028	-0.0028	-0.0029
σ₃	-60.0	-60.0	-60.0
T3	-895 k	-895 k	-1104 k
M3	-59939 k-in	-76042 k-in	-140267 k-in
ε₄	-0.0026	-0.0027	-0.0028
σ₄	-60.0	-60.0	-60.0
T4	0 k	-596 k	-736 k
M4	0 k-in	-47713 k-in	-89830 k-in
phi	0.70	0.70	0.70
N	-12296 k	-14504 k	-18613 k
	-8607	-10153	-13029
Mn	9374 k-ft	15368 k-ft	28830 k-ft
φ-Mn	6562 k-ft	10758 k-ft	20181 k-ft

APPENDIX 4

Point 2

Section	6 x 6	6 x 9.5	6 x 11
c₂	10.00 in	10.00 in	12.00 in
a	8.25 in	8.25 in	9.90 in
.85*f_c	3825.00 psi	3825.00 psi	3825.00 psi
Cc	-2272 k	-2272 k	-2726 k
Rc	5.00	5.00	6.00
Mc	-11360 k-in	-11360 k-in	-16359 k-in
ε₁	0.0171	0.0225	0.0288
σ₁	60.0	60.0	60.0
T1	895 k	895 k	1104 k
M1	50993 k-in	67096 k-in	127014 k-in
ε₂	0.0156	0.0210	0.0275
σ₂	60.0	60.0	60.0
T2	596 k	895 k	736 k
M2	31013 k-in	62623 k-in	80994 k-in
ε₃	-0.0015	-0.0015	-0.0018
σ₃	-43.5	-43.5	-50.8
T3	-649 k	-649 k	-934 k
M3	-3243 k-in	-3243 k-in	-6539 k-in
ε₄	0.0000	0.0000	-0.0005
σ₄	0.0	0.0	-14.5
T4	0.00 k	0.00 k	-178 k
M4	0.0 k-in	0.0 k-in	-356 k-in
phi	0.90	0.90	0.90
N	-1430 k	-1131 k	-1998 k
	-1287	-1018	-1798
Mn	8051 k-ft	12027 k-ft	19272 k-ft
φ-Mn	7246 k-ft	10824 k-ft	17345 k-ft

APPENDIX 4

Pure Bending

Section	6 x 6	9.5 x 14	9.5 x 18
c(bend)	5.79 in	7.38 in	7.43 in
a	4.77 in	6.09 in	6.13 in
.85*f_c	3825.00 psi	3825.00 psi	3825.00 psi
Cc	-1315 k	-1677 k	-1687 k
Rc	2.89	3.69	3.71
Mc	-3804 k-in	-6191 k-in	-6266 k-in
ε₁	0.0317	0.0315	0.0483
σ₁	60.0	60.0	60.0
T1	895 k	895 k	1104 k
M1	54763 k-in	69438 k-in	132065 k-in
ε₂	0.0291	0.0295	0.0463
σ₂	60.0	60.0	60.0
T2	596 k	895 k	736 k
M2	33526 k-in	64965 k-in	84362 k-in
ε₃	-0.0004	-0.0010	-0.0010
σ₃	-11.8	-28.1	-28.4
T3	-176 k	-419 k	-523 k
M3	-139 k-in	-997 k-in	-1270 k-in
ε₄	0.0022	0.0011	0.0010
σ₄	60.0	30.9	30.1
T4	0 k	307 k	370 k
M4	0 k-in	803 k-in	952 k-in
N	0 k	0 k	0 k
Mn	7686 k-ft	11866 k-ft	18743 k-ft
φ-Mn	5380 k-ft	8306 k-ft	13120 k-ft

APPENDIX 4

CAPACITY CALCULATIONS (cont.)

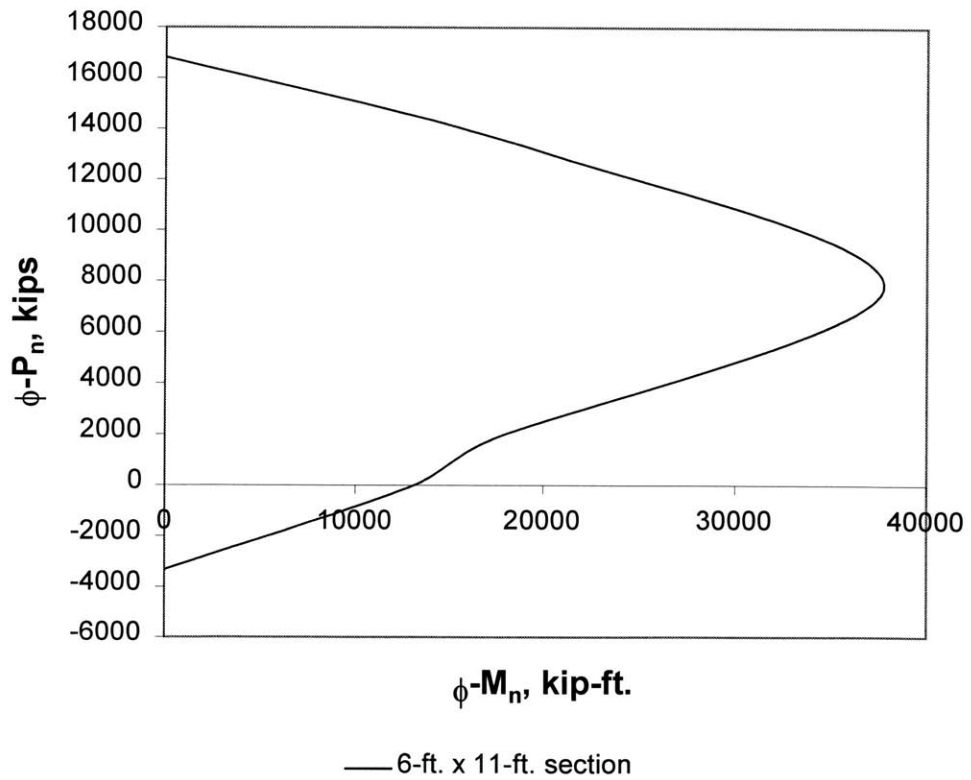
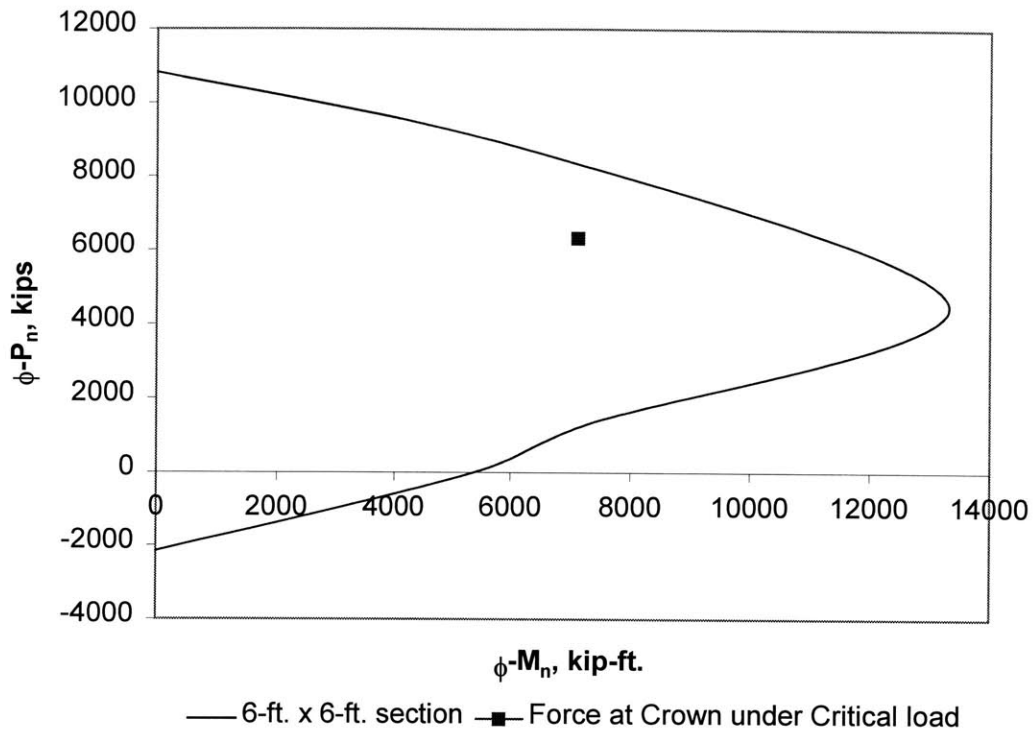
AXIAL COMPRESSION CAPACITY (ref. ACI 10.3.5)

Section	<u>6 x 6</u>	<u>6 x 9.5</u>	<u>6 x 11</u>
ϕ -comp	0.7		
Ag	3888 in ²	4536 in ²	6048 in ²
As	39.76 in ²	54.67 in ²	61.36 in ²
Pn	15470 k	18517	24036
ϕ -Pn	10829 k	12962 k	16825 k

AXIAL TENISON CAPACITY

ϕ -tens	0.9		
Pn	2385.65	3280.26	3681.55
ϕ -Pn	2147.08	2952.24	3313.40

APPENDIX 4



References

- Allen, Edward and Zalewski, Waclaw. Shaping Structures, Statics. New York, New York: John Wiley and Sons, 1998
- Connor, Jerome and Klink, B. Introduction to Structural Motion Control. Cambridge, MA: MIT, 1999
- Heller, Robert and Salvadori, Mario. Structure in Architecture. Englewood Cliffs, New Jersey: Prentice-Hall, 1963
- Leliavsky, Serge. Arches and Short Span Bridges. New York, New York: Chapman and Hall, 1982
- Leontovich, Valerian. Frames and Arches. New York, New York: McGraw-Hill Book Company, 1959
- Melbourne, C. Arch Bridges. London: Thomas Telford, 1995
- Melan, J. Plain and Reinforced Concrete Arches. New York, New York: John Wiley and Sons, 1915
- Nettleton, Douglas A. Arch Bridges. Bridge Division, Office of Engineering, Federal Highway Administration. Washington D.C. : 1977
- Spofford, Charles. The Theory of Continuous Structures and Arches. New York, New York: McGraw-Hill Book Company, 1937